# Semi-empirical schemes for the x-ray mass absorption coefficients used in XRF analysis

JI Xin-Ming, ZHU Jie-Qing, XU Hong-Jie
*(Shanghai Institute of Nuclear Research, the Chinese Academy of Sciences, Shanghai 201800)*

**Abstract** X-ray mass absorption coefficients play an important role in the accuracy of any XRF intensity calculation. It is necessary to determine the proper schemes for providing satisfying values $\mu/\rho$. In this work we examined and compared various schemes. A program based on the existing schemes to provide more accurate and convenient $\mu/\rho$ values was then introduced. The results from the program appears to be tolerable.

**Keywords** X-ray fluorescence (XRF) analysis, Mass absorption coefficients
**CLC numbers** O434, O657.34

## 1 SCHEMES OF X-RAY MASS ABSORPTION COEFFICIENTS

The x-ray fluorescence (XRF) analysis is one of the common non-destructive methods for studying the thickness and the chemical composition of thin film samples. Two general methods have been developed to make the matrix correction, namely the empirical coefficient method (ECM), and the fundamental parameter method (FPM). The ECM uses simple approximated XRF intensity-concentration equations. Its accuracy relies heavily on the equations and the calibration standards used. The FPM uses the basic equation of the x-ray physics directly, and therefore it greatly simplifies the analysis and increases the accuracy. The FPM has been used extensively because it needs less calibration standards than the ECM. Moreover, the FPM has unique advantage, superior to the ECM, for samples with multi-layer films.

The XRF generating process is rather complex. The XRF intensity calculated is affected not only by the peculiarity of the thin film samples, such as the thickness, the composition and the measurement order of the multi-layer thin films, but also by the fundamental parameters. These parameters are the mass absorption coefficients, the absorption edges, the fluorescence yields, the absorption jump factors etc. The accuracy of the XRF intensity calculation is strongly affected by reliable values of the fundamental parameters needed. The mass absorption coefficient $\mu/\rho$ is a function of the x-ray photon energy $E$. There are several experimental databases of the coefficients for all characteristic K-, L- and even M- x-ray lines in form of tables. However, some x-ray spectral analysis based on the multi-channel operation, because of its approximate nature, needs the knowledge of $\mu/\rho$ values for different photon energies in form of formulation. It

---

Manuscript received date: 2001-06-03

is especially important when an x-ray tube is used for XRF excitation. A formulated scheme is needed for the parameters because of the continuing proclivity of the x-ray energy from a tube. Most mass absorption coefficients for XRF were traditionally generated from semi-empirical expressions whose parameters were determined by fitting them to selected experimental data. Several schemes of semi-empirical expressions for mass absorption coefficients exist suiting separately to different x-ray energies and different atomic numbers, and there were some researchers who did some work to rectify the semi-empirical schemes. It is our purpose in this work to determine a unified parameterized scheme for the tube-excited XRF analysis by using FPM method. In this paper, we examine and compare some of these schemes, and present a convenient program to provide $\mu/\rho$ values which are needed for our XRF analysis at the energy region of 0–50 keV.

The equation shown below represents the fundamental theoretical expression for the primary fluorescent x-ray intensity emitted from a bluk of sample.

$$I_i = \text{const} \cdot \frac{\Omega}{4\pi} \cdot k_i \cdot \omega_i \cdot \frac{s_i - 1}{s_i} \cdot p_i \cdot c_i \cdot \int_{E_i}^{E_{\max}} \frac{\tau_i(E) \cdot I(E) \cdot dE}{\frac{\mu(E)}{\sin\theta_1} + \frac{\mu_i(E)}{\sin\theta_2}}$$

where $i$ denotes the considered x-ray lines emitted from different elements, $\Omega$ the solid angle of the detector, $k_i$ the detection efficiency of the detector, $\omega_i$ the fluorescent yield, $s_i$ the absorption edge jump, $p_i$ the transition probability, $c_i$ the weight fraction, $\tau$ the photo-absorption coefficient, $\mu$ the total mass absorption coefficient, $\theta_1$ and $\theta_2$ are the angles of the incident and the observed radiations, and $I(E)dE$ is the primary x-ray intensity hitting the specimen surface with energy from $E$ to $E + dE$.

It is seen that the mass absorption coefficient plays an important role in the calculation of x-ray fluorescent intensity. In general, the absorption coefficient of a material for the x-ray of wavelength $\lambda$ can be calculatd as a sum of the contribution from the composition elements: $\mu_\lambda = \sum_i c_i \mu_{i\lambda}$, where $c_i$ is the weight fraction of element $i$ in the material. The absorption is the sum of a photoelectric part and a scattering part, $\mu_{i\lambda} = \tau_{i\lambda} + \sigma_{i\lambda}$.

Many semi-empirical schemes for mass absorption coefficients are based on the consideration that the photoelectric absorption dominates the coefficient calculation over the Compton and the coherent scattering in the $1-20$ keV energy region. Thus the scattering part is small within the energy region considered. In this case $\mu_{i\lambda} = \tau_{i\lambda}$. Since the photoelectric absorption coefficient has a log-log dependence upon the energy $E$ with the exponent approximate to 3, the basic scheme has a power law expression, like this: $\frac{\mu}{\rho} = CE^{-n}$, Leroux and Thinh,[1] where the constant $C$ is strongly dependent upon the atomic number. For a given element, values of $C$ and $n$ are multipartite, taking specific values between each pair of absorption edges. $E$ is the x-ray energy. According to the standard data collected in Ref.[2], we can reduce the number of parameters by defining a single value $C$ for different elements and fitting it to the variant $CE^{-n}$. The value $C$ and the multiple values of $n$ for various energy intervals between absorption edges (Fig.1) are determined for each element in the x-ray energy region of $0-50$ keV.

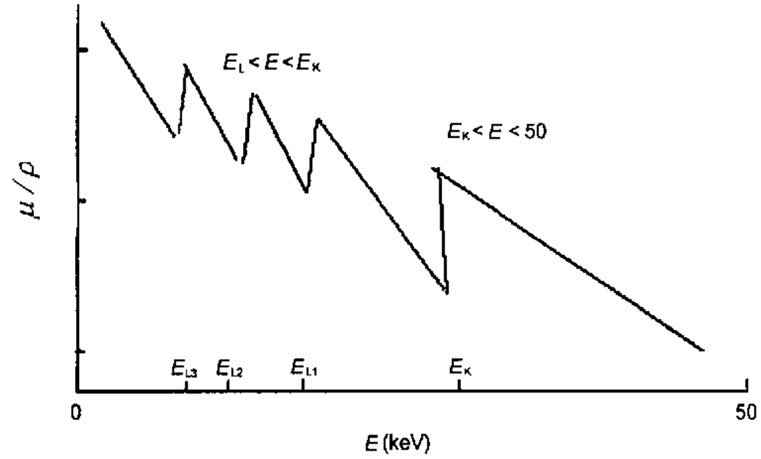

**Fig.1** Schematic diagram indicating the fitting of $\mu/\rho$ over various energy intervals for a given element

However, for attenuation of the higher photon energies in the lightest elements in a sample, the effect of compton scattering is not negligible. A more rigorous approach was introduced by Gerward *et al.*[3] to overcome this deficiency by adding a Klein-Nishina term to describe the scattering into the above power law expression.

Owing to the binding effects, the Klein-Nishina cross-section is not an appropriate description for the incoherent scattering at low energy. In this case, however, the Raylaigh scattering compensates the reduction of Compton scattering due to binding. Then the added Klein-Nishina term can also be used to describe the total scattering at a first approximation. For x-ray energy above the K absorption edge, Gerward's modified power law expression[3] reads like this:

$$\frac{\mu}{\rho} = CE^{-3} + DE^{-4} + \frac{\sigma_{\mathrm{KN}} Z N_{\mathrm{A}}}{A}$$

Here, $Z$ and $A$ are the atomic number and mass of the absorber, $N_{\mathrm{A}}$ is the Avogadro's constant and $\sigma_{KN}$ the electronic Klein-Nishina cross-section.

It is not intended for this paper to be a complete account of all semi-empirical schemes. We merely indicate the problems inherent in the basic power law and some recent developments aiming at rectifying them. The work we did was to select proper semi-empirical coefficient schemes by fitting them to experimental data. In order to achieve an ever better accuracy in calculation of the XRF intensity by FPM method, expressions of mass absorption coefficients for the 50 kV tube excited XRF analysis were formed based on those existing semi-empirical schemes, in which Gerward's expression of the basic power law with a scattering term (PL+S) was used, and quadratic and cubic correction were introduced for rectification, then a program was made up of these ingredients to provide unifyingly the mass absorption coefficient being used in XRF analysis.

## 2 FITTING AND THE RESULTS

In the work, most of the semi-empirical expressions described above were fitted to a large volume of experimental data collected by De Boer[2] of Philips Research Laboratories (PRL). In order to determine the best expressional parameters for all elements and identify the appropriate schemes used for XRF analysis, copper and silver were selected as examples to examine the schemes and compare the results of their fitting in the x-ray energy region 0−50 keV. A non-linear least-squares code was used to fit the expressions chosen and their parameters were extracted afterwards. Considering the fluctuations close to the absorption edges, the fitting for all absorbing elements were carried out separately in different intervals, i.e., by subdividing the x-ray energy region into segments between absorption edges.

In the program, the above mentioned schemes were adopted, and according to the recent developments, quadratic and cubic corrections were also introduced for rectifying the results. The following equations were used in our program.

$$\frac{\mu}{\rho} = p_1 E^{-3} + p_2 E^{-4} \tag{1}$$

$$\frac{\mu}{\rho} = \sum_{i=0}^{i=3} p_{i+1} (\ln E)^i \tag{2}$$

$$\frac{\mu}{\rho} = \exp[p_1 + p_2 \ln E + p_3 (\ln E)^2] \tag{3}$$

$$\frac{\mu}{\rho} = \exp[p_1 + p_2 \ln E + p_3 (\ln E)^2 + p_4 (\ln E)^3] \tag{4}$$

Eq.(1) is the basic power law of Gerward[3] (marked as PL). Eq.(2) (marked as LC) is a log cubic correction that is derived from PL to rectify the results in low enery 0–1 keV.[4] Eq.(3) attempts to account for the departure of the curve of $\ln(\mu/\rho)$ versus $\ln E$ from a pure linear dependence by introducing a quadratic correction[5] (marked as PLQC). Eq.(4) (marked as PLCC) extends to a cubic correction. While we have to take into account the effect of scattering, a Klein-Nishina scattering term was added to each of the sets of Eqs.(1)–(4) (This procedure is marked as +S in each case).

Table 1 collects all the results from these fittings. The root-mean square (rms) deviations between the fitting curves and the experimental values from De Boer[2] (PRL) and the index parameters $p_2$ are presented in the table. Figs. 2 and 3 show the results of fitting for copper and silver.

**Table 1** Root-mean square deviation (rms) between the PRL $\mu/\rho$ values and the values obtained by fitting semi-empirical expressions. The values of the index parameters $p_2$ are results from fits of Eqs.(1)-(4).

| Equation | Symbol | rms for Cu ($E > E_K$) | $\mid p_2 \mid$(Cu) | rms for Ag ($E_{L1} < E < E_K$) | $\mid p_2 \mid$(Ag) |
|---|---|---|---|---|---|
| **(1) | PL+S | 0.6776 | * | 3.0032 | * |
| (2) | LC | 0.18487 | * | 30.25574 | * |
| (3) | PLQC | 0.20786 | 2.1730 | 3.206801 | 2.5829 |
| **(3)+S | **PLQC+S | 0.18604 | 2.0576 | 3.20019 | 2.5387 |
| (4) | PLCC | 0.18486 | 1.4825 | 3.1987 | 2.7203 |

*$p_2$ should be ignored while the scattering was not taken into account.

**In case the scattering term was added in the fitting, +S symbol is marked.

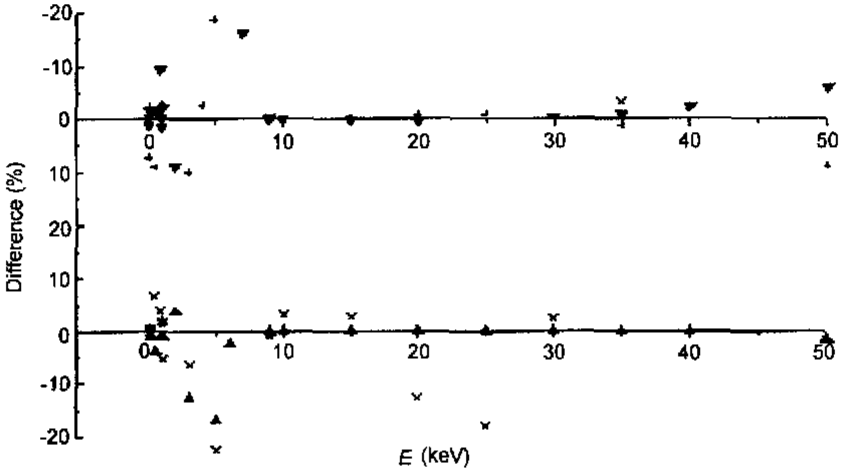

**Fig.2** Percent differences between the experimental data from PRL and the values obtained by fitting the expression in program for copper.

Here, + Eq.(1) (PL+S), × Eq.(2) (LC), ▼ Eq.(3) (PLQC), ▲ Eq.(4) (PLCC)

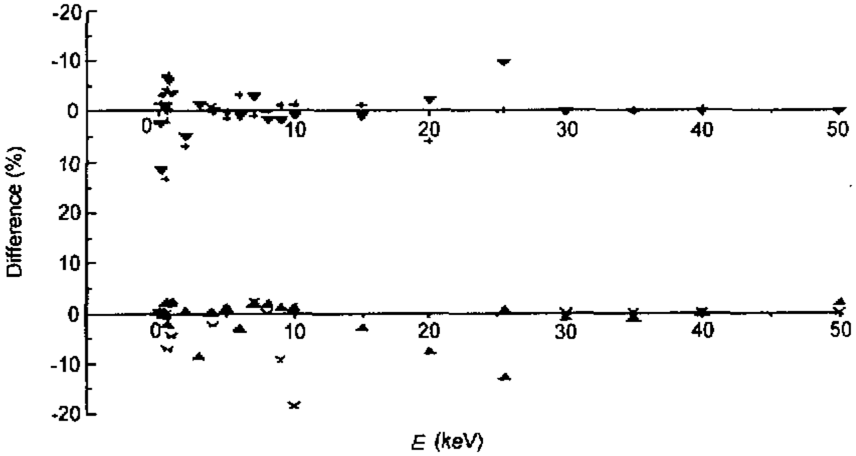

**Fig.3** Percent differences between the experimental data from PRL and the values obtained by fitting the expression in program for silver.

Here, + Eq.(1) (PL+S), × Eq.(2) (LC), ▼ Eq.(3) (PLQC), ▲ Eq.(4) (PLCC)

The PLQC and PLCC served well in energy region $E > E_K$. Their rms are 0.20786, 0.18486, respectively. The PLCC is better than PLQC. Their results are shown in Fig.4. The PLCC reduced all deviation to lower than 1% in $E > E_K$. Both of the PLQC and the PLCC did not give excellent outcomes covering the entire energy region because they encountered problem while closing to the absorption edges, as shown in the figures. The discrepancy even exceeds 20% for silver. For silver, the rms deviation of PLQC and PLCC reach 3%. It is due to the errors growing greatly near the junction of the jumping regions.

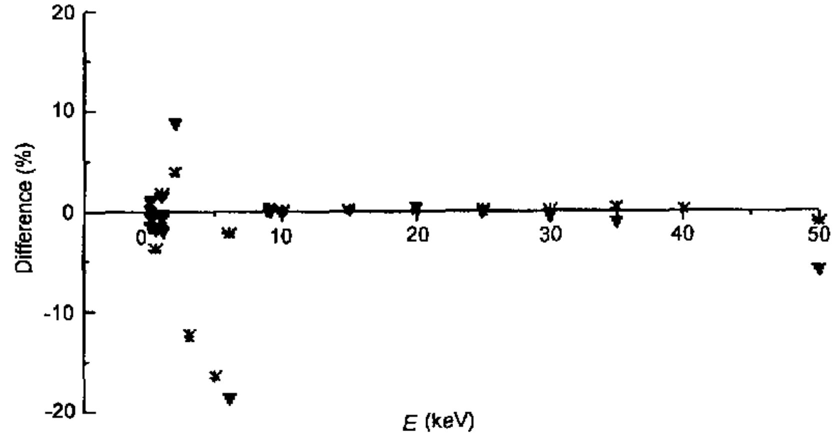

**Fig.4** Fitting results of Eq.(3) in comparision with the results of Eq.(4) for copper. Here, ▼ Eq.(3) (PLQC), * Eq.(4) (PLCC)

In Fig.5 we compare the results of PLQC including the Klein-Nishina scattering term with the results of PLQC without the scattering. It shows that the correction for scattering is necessary, especially for the light elements, where the scattering contributes a significant fraction for $\mu/\rho$.

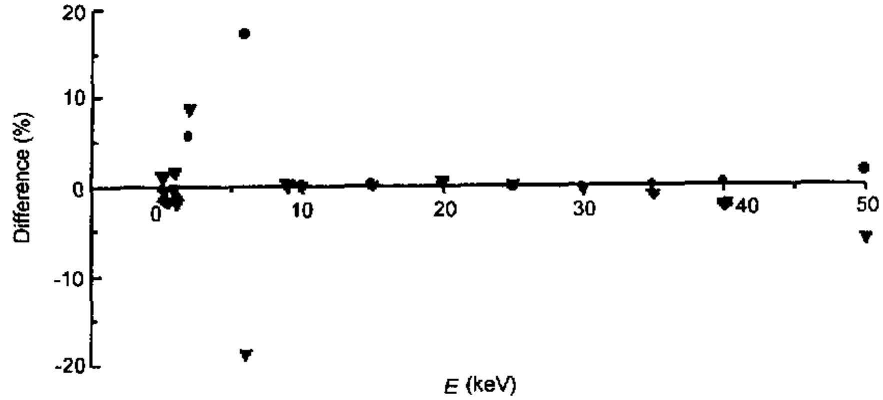

**Fig.5** Comparison of the results from Eq.(3) (PL quadratic correction) and Eq.(3)+S (PLQC + scattering term) for copper. Here, ▼ PLQC, ● PLQC+S

In our program we chose LC, Eq.(2), in low energy region 0−1 keV because it could provide excellent agreement. The results are shown in Fig.6. Attentions must be paid to the variation in the index parameter $p_2$, which reflects the low energy scattering by a separate term as shown in Table 1.

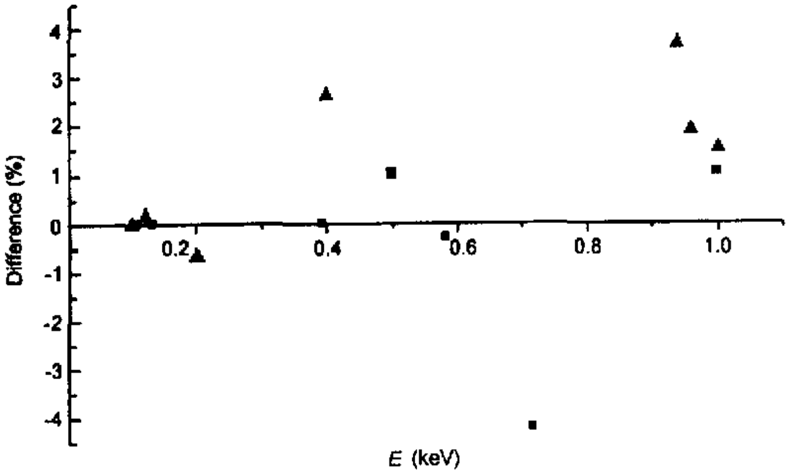

**Fig.6** Fitting results of Eq.(2) (LC) in 0 1keV energy region for copper and silver. Here, ■ for the results of copper, ▲ for the results of silver

For the fitting, which ignored the scattering term, a higher rms deviation value was obtained. For the fitting that included the scattering term, a much lower rms deviation value was achieved. It indicates the distortion arose when one described the photoelectric plus scattering processes only by the PL scheme. Table 2 shows some representative parameters from the fitting of these equations.

**Table 2** *Parameters from fittings of the Eqs (3), (3)+S and (4) to the PRL values*[2] *of* $\mu/\rho$ *for* copper and silver

| Element | Energy region(keV) | Eq | $p_1$ | $p_2$ | $p_3$ | $p_4$ |
|---|---|---|---|---|---|---|
| Cu | $E > E_K$ | (3) | 10.9653 | -2.17303 | -0.1035 | |
| | | (3)+S | 10.8299 | -2.05764 | -0.1286 | 0.3429 |
| | | (4) | 10.3633 | -1.48254 | -0.3651 | 0.0326 |
| Ag | $E_{L1} < E < E_K$ | (3) | 10.9321 | -2.5829 | -0.0371 | |
| | | (3)+S | 10.8993 | -2.53874 | -0.05233 | 1.1755 |
| | | (4) | 11.0109 | -2.72032 | 0.04081 | -0.0144 |

## 3 CONCLUSION

The program being used to fit absorption coefficients for all elements was subdivided into several segments according to the x-ray energy intervals between the absorption edges. The results can be summarized as follows.

(i) $E > E_K$. The schemes of PL+S, PLQC+S and PLCC are all fitted well for 10< $Z$ <50. The PLCC provides excellent fittings with rms deviation less than 0.2% in general. However, for the higher $Z$ values ($Z$ >40), where the width of the energy interval for fitting is small, the PLCC correction seems unnecessary. At this time, the scheme of PL+S is sufficed in each case with rms deviation <0.25%.

(ii) $E_{L1} < E < E_K$. Here, the atomic number region is $11< Z <85$. At low $Z$ region, where the energy is low, the PL+S scheme is sufficed. When $Z$ is above 20, the PLQC scheme including a scattering term and the PLCC scheme displayed well. Their rms deviations are invariably below 3.2%.

(iii) $E_M < E < E_{L3}$. At the low $Z$ region, $20< Z <30$, the LC scheme is sufficed. When $Z$ is above 30, the PLQC scheme is acceptable. Their rms deviations are below 1.5%.

It is necessary to determine the $\mu/\rho$ values by a unified scheme for the use in the calculation of x-ray intensity by FPM method, especially for the case of tube excited XRF analysis and the analysis of specimen with multi-layer films. We have tested and compared some existing semi-empirical schemes about their capabilities to describe the $\mu/\rho$ values. It has been proven that this program provides a convenient calculation of $\mu/\rho$ values for a wider energy region. The program can give a fairly good agreement with the standard data by choosing different expression according to different atomic number and energy interval. However, it is not perfect especially near the regions where the mass coefficient has a jump.

## References

1 Leroux J, Thinh T P. Revised tables of mass attenuation coefficients. Quebec: Corporation Scientifique Classe, 1977, **212**:427

2 De BOER D K G. Philips Res Lab, Spectrochem Acta, 1989, **44B**(11):1171

3 Gerward L. X-ray Spectrom, 1986, **15**:29

4 Manter M. In: Gilgrich J V *et al* ed. Advances in x-ray analysis (New York: Plenum Press), 1993, **36**:27−33

5 Gampbed J L, DeForge D. X-ray Spectrom, 1989, **18**:235-242